

# Dualband Spectral-Spatial RF Pulses for Prostate MR Spectroscopic Imaging

Amir A. Schricker,<sup>1</sup> John M. Pauly,<sup>2</sup> John Kurhanewicz,<sup>1</sup> Mark G. Swanson,<sup>1</sup> and Daniel B. Vigneron<sup>1\*</sup>

**Although MR spectroscopic imaging (MRSI) of the prostate has demonstrated clinical utility for the staging and monitoring of cancer extent, current acquisition methods are often inadequate in several aspects. Conventional 180° pulses can suffer from chemical shift misregistration, and have high peak-power requirements that can exceed hardware limits in many prostate MRSI studies. Optimal water and lipid suppression are also critical to obtain interpretable spectra. While complete suppression of the periprostatic lipid resonance is desired, controlled partial suppression of water can provide a valuable phase and frequency reference for data analysis and an assessment of experimental success in cases in which all other resonances are undetectable following treatment. In this study, new spectral-spatial RF pulses were developed to negate chemical shift misregistration errors and to provide dualband excitation with partial excitation of the water resonance and full excitation of the metabolites of interest. Optimal phase modulation was also included in the pulse design to provide 40% reduction in peak RF power. Patient studies using the new pulses demonstrated both feasibility and clear benefits in the reliability and applicability of prostate cancer MRSI. Magn Reson Med 46: 1079–1087, 2001. © 2001 Wiley-Liss, Inc.**

**Key words:** RF pulse design; MR spectroscopic imaging; spectral localization; prostate cancer; magnetic resonance imaging

Recently, 3D magnetic resonance spectroscopic imaging (MRSI) studies have demonstrated clinical utility for determining the location and spatial extent of cancer within the prostate (1–3) and its spread outside the gland (4). Prostate cancer can be metabolically identified with high specificity by an elevation in the choline-to-citrate peak area ratio relative to normal prostatic tissues. The high specificity of MRSI complements the high sensitivity of MRI for identifying cancer, and MRSI is now used routinely in clinical/research MR staging exams at our institution to provide a combined anatomic/metabolic assessment of prostate cancer extent. For the combined MRI/MRSI prostate exam to be accepted in general clinical practice, robust acquisition techniques must be developed and implemented. The conventional point-resolved spectroscopy (PRESS) (5–7) technique is often limited by inadequate water or lipid suppression and chemical shift misregistration.

Spectral-spatial excitation pulses (8–11) have demonstrated the ability to address these problems (8,12). This type of RF pulse excites a slice, but only at a specific range of frequencies. They are also known as echo-planar spin-echo (EPSE) pulses, because they use a gradient waveform that is essentially the same as echo-planar imaging (EPI). The spectral-spatial PRESS sequence uses two EPSE 180° pulses to define both spatial and spectral profiles (8). However, the complete suppression of the water resonance provided by these pulses is undesirable for clinical MRSI since residual water signals can serve as valuable references for phase and frequency correction. The detection of residual water in each voxel is also critical for monitoring treatment response. Following hormone ablation or radiation therapy, choline, creatine, and citrate levels can decrease to noise levels (1,2). In these cases, the observation of residual water provides assurance that cellular atrophy, not a hardware or software error, resulted in the detection of no metabolite resonances.

Another RF excitation problem commonly facing prostate MRSI studies is the peak power limitation inherent in body coil transmission. RF pulses with the necessary spatial selectivity have high peak power requirements, which in many large patients can exceed the RF power limit. Reducing the peak power of these pulses is critical for the widespread clinical applicability of prostate MRSI. Recently, methods have been developed for designing nonlinear phase pulses with reduced peak power (13–15). These pulses have been applied for high-bandwidth, high-selectivity spatial suppression pulses for MRI (15) and MRSI (21), but not for 180° excitation pulses. The goal of this study was to develop new dualband EPSE 180° pulses in order to: 1) provide a low-level excitation of the water resonance; 2) exclude excitation of the lipid resonances; 3) fully excite the creatine, choline, and citrate resonances; and 4) add optimal nonlinear phase-modulation to the spectral-spatial pulses to minimize peak power.

## METHODS

### Pulse Design

The frequency passband for detecting prostatic metabolites at 1.5T was designed to pass a range of frequencies from the choline resonance at 3.2 ppm (96 Hz, referenced from water) to the citrate resonance at 2.6 ppm (120–140 Hz), while not exciting lipids below 1.6 ppm (200 Hz). A second passband of approximately 100 Hz was centered about water. The 10% amplitude of this band was designed to attenuate water by a factor of 100 after the two 180° pulses in the PRESS sequence. Frequencies greater than 50 Hz downfield of the water peak were designed to be not excited by these pulses.

<sup>1</sup>Department of Radiology, University of California–San Francisco, San Francisco, California.

<sup>2</sup>Department of Electrical Engineering, Stanford University, Palo Alto, California.

Grant sponsor: National Institutes of Health; Grant numbers: RO1 CA59897; RO1 CA79980; R33 CA88214; Grant sponsors: GE Medical Systems; CaP CURE Foundation.

\*Correspondence to: Daniel B. Vigneron, Ph.D., Magnetic Resonance Science Center, Department of Radiology, Box 1290, University of California–San Francisco, San Francisco, CA 94143-1290. E-mail: vigneron@mrs.csf.edu

Received 6 April 2001; revised 17 July 2001; accepted 18 July 2001.

Spectral-spatial EPSE pulses consist of a series of subpulses, each applied during one sublobe of an oscillating gradient. These were designed using an extension of the method outlined by Pauly and coworkers (11). Using the Shinnar Le-Roux (SLR) algorithm for RF pulse design (16–20), the effect of each EPSE pulse was described by a pair of complex polynomials ( $\alpha(k_z, k_\omega)$ ,  $\beta(k_z, k_\omega)$ ). One polynomial,  $\beta$ , is proportional to  $\sin(\phi/2)$ , where  $\phi$  is the flip angle. The second polynomial is  $\alpha$ , and in this case it is completely determined once  $\beta$  is determined (20). The 2D  $\beta(k_z, k_\omega)$  is designed by choosing a spectral profile and a spatial profile. The RF pulse is produced by inverting the SLR transform first in the spectral (nonlinear) axis, and then in the spatial axis. The spatial subpulses are small-tip angle rotations, so a linear design suffices in this axis. These subpulses produce the spatial selectivity of the EPSE pulse. Conceptually, the amplitude of the subpulses are multiplied by an envelope, which defines the spectral profile of the EPSE pulse. In practice, a full 2D inverse SLR design (11) was used, which gives a higher-fidelity selective profile. The PRESS spectrum is given in terms of the transforms of these two polynomials:

$$S(z, \omega) = (\beta_1^*(z, \omega))^2 (\beta_2(z, \omega))^2. \quad [1]$$

Since the two  $180^\circ$  pulses are identical, the spectrum  $S(z, \omega) = |\beta(z, \omega)|^4$ . Hence, the  $\beta(z, \omega)$  profile was designed to be the fourth root of the desired SE profile.

To produce the dualband EPSE pulse, we started with a dualband profile in the spectral axis of  $\beta(k_z, k_\omega)$ . To create this dualband spectral profile, a complex, dualband digital filter was designed in Matlab (Math Works Inc., Natick, MA) The RF pulse design tools (supported by NIH Research Resource Grant P41 RR09784) are available on the internet (zoyd.stanford.edu), and this dualband pulse is provided as a design example. As shown by Star-Lack et al. (8), even if the spectral phase profile of each pulse is nonlinear, by using two identical  $180^\circ$  pulses the nonlinear profiles exactly compensate each other, thereby producing a linear phase, completely refocused echo. Since the phase profiles of the two  $180^\circ$  pulses compensate each other, a maximum-phase design can be used to minimize the spectral transition width (20). This was done by designing a linear-phase, equal-ripple filter, and then decomposing it into minimum- and maximum-phase components (20). The key issues in the design of this pulse were the specifications of the band edges and transition widths. The passband edges were determined by the location of metabolite signals. An initial value for the transition width was calculated by methods outlined by Pauly et al. (20) for calculating these same parameters in single band pulses. The design equation for single band pulses that relates transition bandwidth, pulse duration, and ripple amplitudes is (adapted from Ref. 20):

$$D_\infty(\delta_1, \delta_2) = T^* BW \quad [2]$$

where  $D_\infty$  is a function of the in-slice and out-of-slice ripple amplitudes  $\delta_1$  and  $\delta_2$ ,  $T$  is the length of the pulse, and  $BW$  is the width of the transition band. The initial transition width was computed from these parameters.

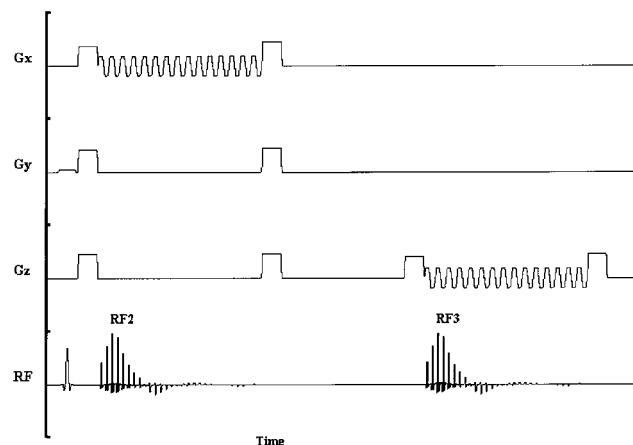


FIG. 1. Modified PRESS sequence with two dualband minimum-phase EPSE pulses (RF2 and RF3) applied in the x and z directions. The amplitude of the waveform is displayed on the “RF” line, with the gradient waveforms displayed on the lines labeled Gx, Gy, and Gz.

The remaining Parks-McClellan parameters for the digital filter were calculated as follows. Over the attenuated passband, the slice profile was specified to be 0.10, yielding an overall water attenuation of 100-fold when both  $180^\circ$  EPSE pulses were applied. Finally, the initial ripple amplitude parameters were set at 0.010 (stopband), 0.001 (attenuated passband), and 0.001 (unity passband).

### Pulse Optimization

All initial parameters were determined based on the single band design, and then were interactively optimized to achieve the following criteria: 1) water signal suppression by a factor of 100 in the downfield stopband, 2) lipid suppression by at least a factor of 1000, 3) less than 2% passband ripple, and 4) less than 5% ripple in the attenuated passband. Since there was greater latitude in water suppression, the requirement on the attenuated passband ripple was less stringent than that for the metabolite passband. Tradeoffs between the parameters were determined empirically. Increased passband width led to increased peak RF power and increased passband ripple. Furthermore, the minimum passband width was determined by the frequency range of the metabolite resonances of interest. The transition width determined by Eq. [2] was used as a minimum value, since widths less than that value led to an observable increased out-of-slice ripple. Optimal design values resulted from modifying the passband widths while keeping a fixed transition width. In the optimized pulse design, the water band extended from  $-159$  Hz to  $-83$  Hz, and the full passband extended from  $-34$  Hz to  $+38$  Hz. The downfield stopband began at  $-186$  Hz, and the upfield stopband began at  $+80$  Hz.

Once the spectral profile was designed, the next step was the choice of spatial profile. The number of sublobes was determined by the requirement that the  $N/2$  excitation sidelobes not contaminate the desired spectral stopbands. In this case we used 1.2-ms sublobes, so that the sidelobes were centered at  $\pm 416$  Hz. Two constraints limited the spatial profile: 1) the gradient area that could be applied

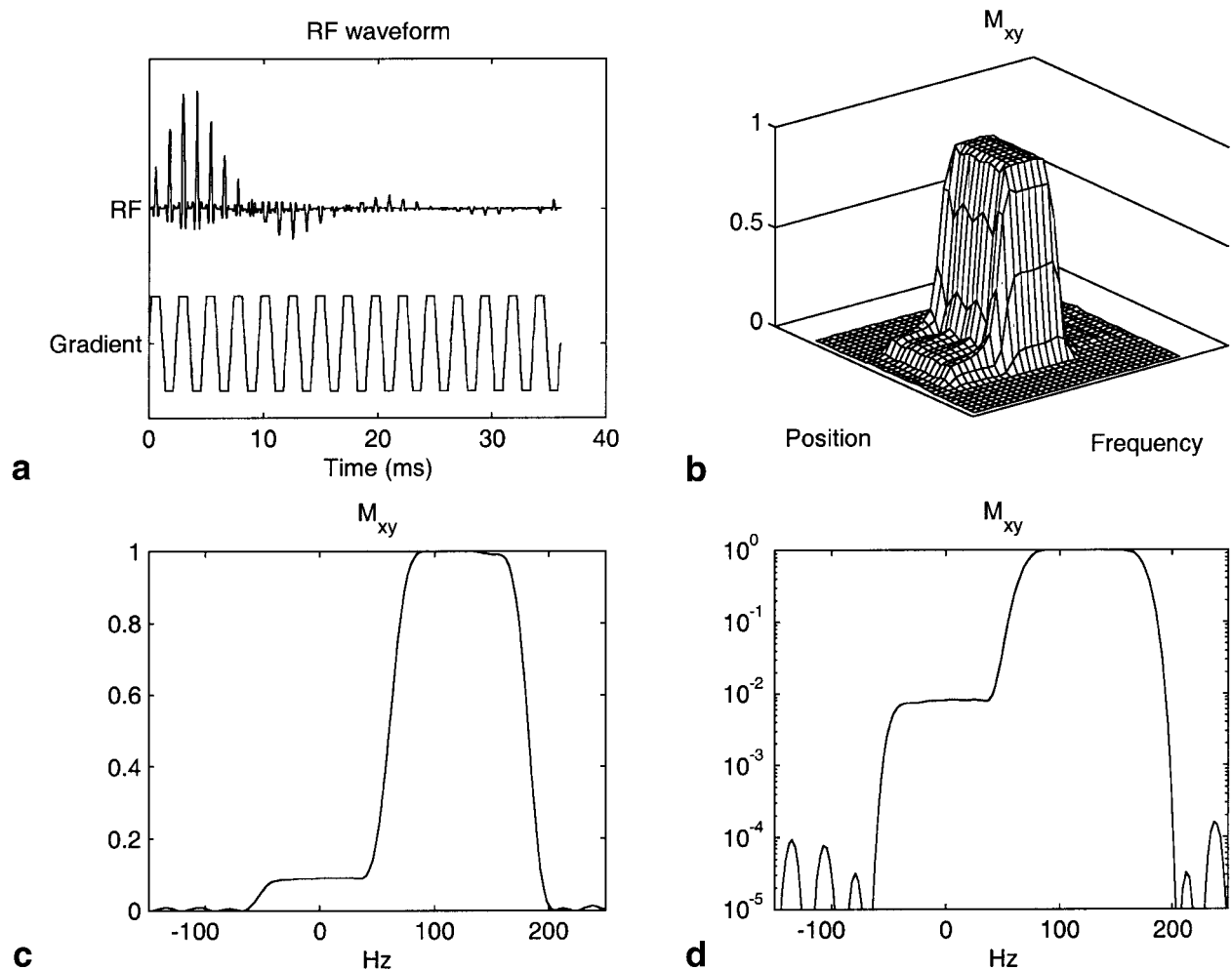


FIG. 2. **a:** RF and gradient waveforms of the maximum-phase dualband EPSE pulse. **b:** 2D spectral-spatial excitation profile after one application of the dualband pulse. Minimal stopband ripples in the frequency dimension and negligible ripples in the spatial dimension are evident. **c:** Frequency profile after one application of the dualband pulse. **d:** Semi-log plot of the frequency profile after two applications of the dualband pulse, as required for PRESS. Theoretical water attenuation is 100-fold. The passband includes resonances ranging from choline to citrate. The stopband includes lipids and shows a theoretical lipid suppression higher than  $10^4$ .

during the 1.2-ms sublobes, which limited the minimum volume that could be excited; and 2) the peak RF power that would be required. As the subpulses become more selective, the peak power increases. The spatial profile is determined by the time-bandwidth product, which is the duration of the pulse multiplied by its passband width. In order to keep an acceptable overall peak RF power, the time-bandwidth product of the subpulses was chosen to be 7.2. With a 1.2-ms subpulse duration, this corresponded to a bandwidth of 6 kHz. With the 4.0 G/cm gradients, this allowed PRESS volumes as small as 3.5 mm on a side, which is much smaller than required. Hence, the gradient system was not a limitation for these pulses.

A second phase-modulated dualband pulse with less peak power requirements was also designed. For a given slice profile, a conventional linear phase pulse generally requires the highest peak power of any pulse with that same magnitude profile. Minimum- and maximum-phase pulses are only slightly better. By introducing phase into the profile, the peak RF power can often be reduced dra-

matically, usually by the square root of the time-bandwidth product. To produce the minimum peak power pulse, we alternately flipped combinations of the passband zeros of the maximum phase  $\beta$  and searched for the minimum peak power. Using custom Matlab design tools, phase modulation was introduced in the spectral dimension, and a new pulse was created which had the same profiles as the original pulse, but with reduced peak RF amplitude. Since the RF power is reduced, the spatial selectivity could be improved by using a higher time-bandwidth in the spatial dimension.

#### Phantom Studies

Ten phantom MRSI experiments were performed to test the new dualband EPSE PRESS sequence against conventional PRESS sequences. A modified PRESS excitation pulse-sequence was created which incorporates the two identical phase-modulated dualband spectral-spatial EPSE pulses (Fig. 1).

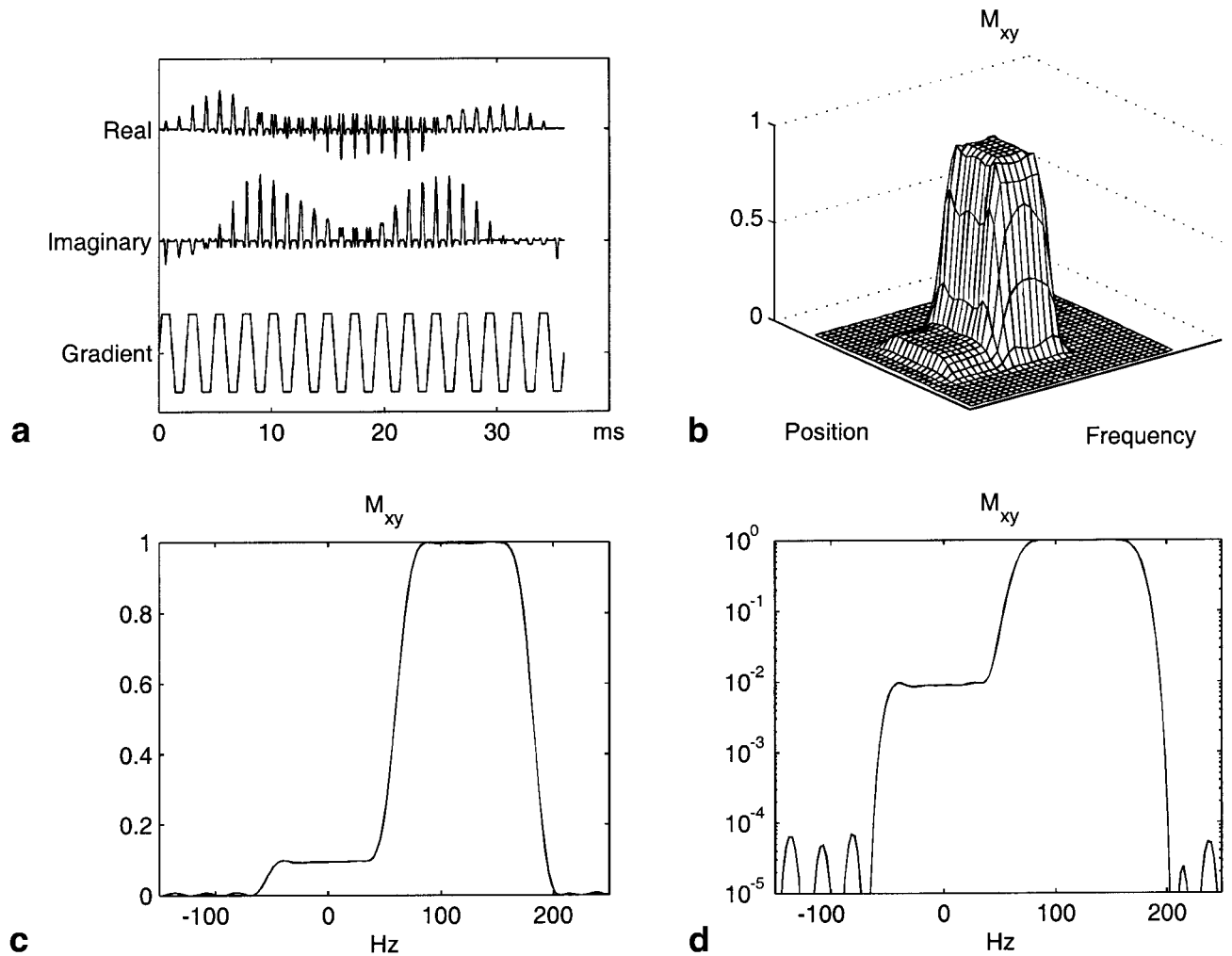


FIG. 3. **a:** RF (real and imaginary components) and gradient waveforms of the quadratic phase modulated version of the dualband pulse. **b:** Magnitude 2D spectral-spatial excitation profile after one application of the phase-modulated dualband pulse. Minimal stopband ripples in the spectral dimension are evident. **c:** Frequency profile after one application of the phase-modulated dualband pulse. **d:** Semi-log plot of the frequency profile after two applications of the phase-modulated dualband pulse, as required for PRESS. Spectral profile is nearly identical to that of the nonmodulated pulse.

All experiments were performed on a GE 1.5T Signa MR imager with spectroscopy capability and 4.0 G/cm gradients (General Electric Medical Systems, Milwaukee, WI). The body coil was used for excitation, and signal reception was provided by an endorectal coil (Medrad Inc., Pittsburgh, PA) combined with a pelvic phased-array coil. A phantom solution was made to represent approximate physiologic concentrations of the major prostatic metabolites. Choline (4 mM), creatine (10 mM), citrate (33 mM), and lactate (12 mM) were dissolved in 600 mL of water and transferred to a 10-cm-diameter plastic sphere.

Two sets of PRESS MRSI spectra were acquired in each phantom exam to compare the new dualband scheme with existing methods employing the band-selective inversion with gradient dephasing (BASING) water suppression scheme (22). The data acquisition parameters for all phantom experiments were TE = 130 ms, TR = 1 s,  $8 \times 8 \times 8$  phase-encoding steps, MRSI resolution =  $1.00 \text{ cm}^3$ , and total scan time = 8.5 min. The PRESS box size was  $60 \times 60 \times 40 \text{ mm}^3$ . No spatial suppression pulses were used in the phantom MRSI experiments.

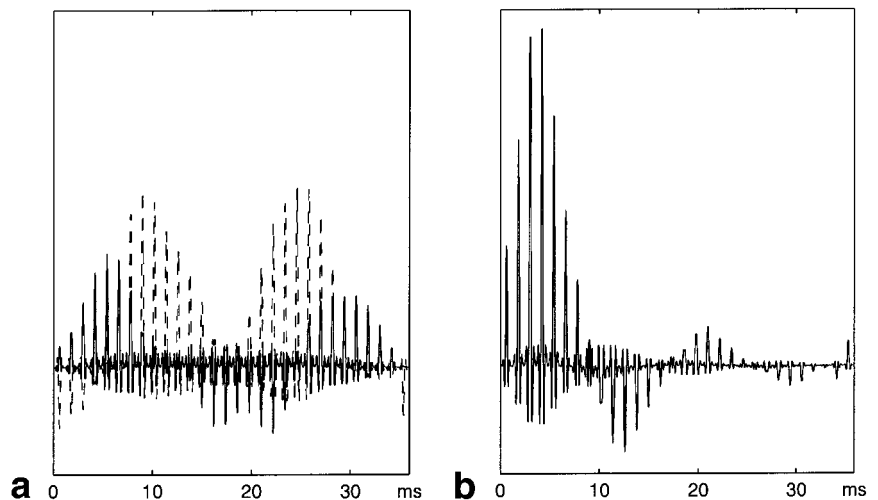
#### Patient Studies

Research MRI/MRSI exams employing the new dualband pulses were performed on five prostate cancer patients. Following routine diagnostic MRI, SI data was obtained first with the BASING sequence and then with the dualband EPSE sequence in three patients and with the dualband scheme alone in two patients. Identical PRESS boxes were selected for both BASING and EPSE acquisitions. The PRESS sequence used in the patient studies included a train of very selective saturation (VSS) prepulses (21) separated by crusher gradients to provide spatial suppression to null periprostatic lipids. Data acquisition parameters for all patient MRSI exams were TE = 130 ms, TR = 1000 ms,  $16 \times 8 \times 8$  phase-encoding steps, MRSI resolution =  $0.34 \text{ cm}^3$ , and total scan time = 17 min. The PRESS box size was typically approximately  $50 \times 25 \times 30 \text{ mm}^3$ .

#### Data Analysis

All 3D MRSI spectral data were reconstructed offline on a Sun UltraSparc 10 system. The MR images were analyti-

FIG. 4. Comparison of phase-modulated and nonmodulated dualband pulses. **a:** Overlaid real (solid) and imaginary (dashed) waveforms of the phase-modulated pulse. **b:** RF waveform of the nonmodulated pulse, plotted on the same scale. The peak amplitude of the phase-modulated pulse is 40% lower than for the nonmodulated version.



cally corrected for the reception profile of the endorectal coil (1,23). The spectra were apodized with a 1 Hz Gaussian filter and Fourier transformed in the time and three spatial dimensions. Software developed in our laboratory was used to automatically frequency align, phase and calculate peak height, area, and signal-to-noise ratio (SNR) for each spectral resonance. The corrected MR images and 3D MRSI data were aligned and displayed using custom-designed IDL tools (Research Systems, Inc., Boulder, CO) which presented the MRSI grids and location of the PRESS box overlaid on the MR images. Following zero-filling in the time domain, spectral analysis was performed in the frequency domain using peak area integration over the width of each spectral region (choline: 12 points; creatine: 8 points; and citrate: 19 points) with no line-shape assumptions. The data were analyzed to determine the amount of water suppression, compare the SNR of each metabolite peak obtained with the new pulses with those acquired with current acquisition methods, and to determine the degree of chemical shift misregistration errors. To quantify the effects on spectral peak intensities due to these frequency-induced spatial displacements, we compared the (choline + creatine)/citrate (CC/C) ratio of the voxels on the left and right edges of the  $6 \times 6$  spectral arrays acquired with both the dualband and BASING pulses. In the three patients for whom MRSI data was acquired with both the dualband and the conventional  $180^\circ$  pulse BASING method, peak area ratios were compared between the two datasets.

## RESULTS

### Pulse Design

The final optimized pulse is shown in Fig. 2; the spectral profile of the SE produced by the PRESS sequence using a pair of these pulses is also plotted in one and two dimensions. The 36-ms maximum-phase pulse was produced with the following design parameters: 1.2 ms per sublobe, 30 sublobes, and a spatial time-bandwidth product of 7.2. The slice profile provided full intensity for the choline, creatine, and citrate passband, but only 10% excitation over the water band. The metabolite passband had a

width of 84 Hz, which allowed for  $+25/-15$  Hz  $B_0$  inhomogeneities before 5% attenuation of the passband metabolites occurred. The magnitude of the passband ripple was less than 1.5%. The attenuated passband had a width of 80 Hz. Frequencies corresponding to the lipid signals were suppressed by a factor of approximately 1000.

The phase-modulated pulse waveforms and gradients are plotted in Fig. 3. The frequency profile was identical to that for the nonmodulated pulse. The peak RF power for the nonmodulated pulse was 0.20G (0.83 kHz). Phase modulation of the original pulse resulted in a 40% reduction of peak RF power, to 0.12G (0.51 kHz), and experimental results confirmed this power reduction. The plot of the phase-modulated pulse demonstrated the same area as the nonmodulated pulse waveform, but the maximum amplitude was greatly reduced (Fig. 4).

### Phantom Studies

Figure 5 shows sample voxels from phantom spectroscopy studies using the dualband scheme. The data were successfully phased with a zero-order correction indicating that the two minimum-phase EPSE pulses yielded a linear phase spectrum when incorporated into the PRESS sequence. Overall, water was suppressed by a factor of 100. The mean SNR of choline for this data set was 5.2 for the dualband scheme and 4.4 for the BASING scheme, performed in the same exam.

Phantom tests demonstrated the intended degree of water suppression while leaving metabolite intensities unaffected. Also, chemical shift misregistration was greatly reduced by using the dualband spectral-spatial pulses. For the acquisition with conventional  $180^\circ$  pulses, the mean CC/C ratios for voxels on the left edge of the PRESS box exhibited substantial differences from those on the right, which was not the case for the dualband pulse scheme. To assess this effect, the mean CC/C intensity ratios for the voxels on opposite edges were calculated for both phantom data sets. For the conventional PRESS acquisition with BASING water/lipid suppression, the voxels on the left edge demonstrated a lower CC/C ratio ( $0.698 \pm 0.233$ ) than those on the right edge ( $CC/C = 0.929 \pm .505$ ). How-

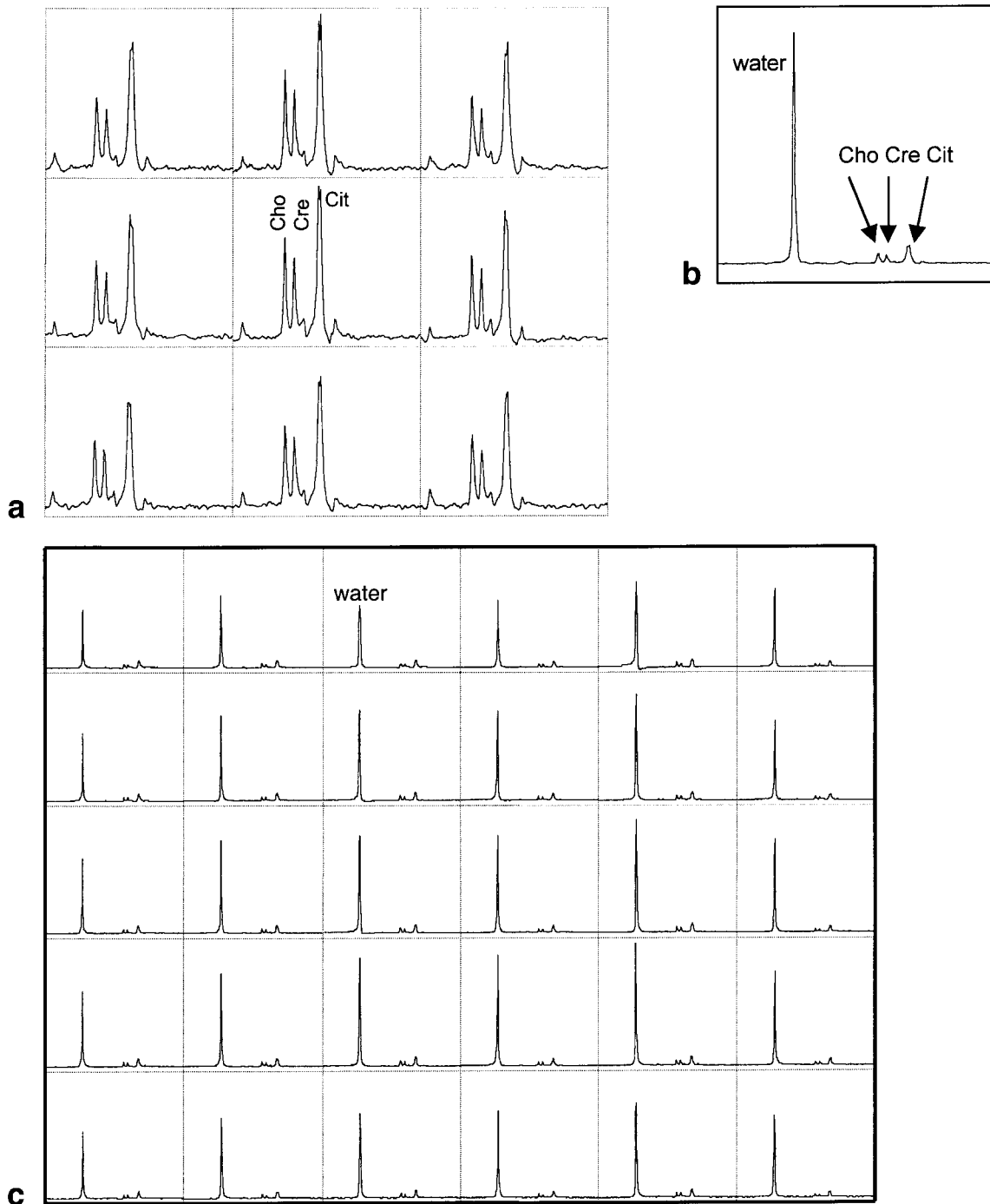


FIG. 5. MRSI of phantom solution. **a:** 1 cc MRSI voxels acquired with the dualband EPSE pulse in a phantom containing 4 mM choline (Cho), 10 mM creatine (Cre), and 33 mM citrate (Cit). **b:** The residual water peak remaining in each voxel, at 100 $\times$  attenuation, was approximately 10 times more intense than the citrate peak. **c:** The 5  $\times$  6 grid from which spectral data were acquired, displaying a uniform residual water peak within the PRESS box.

ever, virtually identical edge ratios with much lower standard deviations were observed in the dualband data set, with the average left edge CC/C =  $0.685 \pm 0.020$  and the average right edge CC/C =  $0.691 \pm 0.079$ . The dualband pulse scheme produced uniform spectra across the PRESS selected region with peak areas all identical within experimental error.

#### Patient Studies

Diagnostic-quality MRSI data were acquired for all five patient exams using the new RF pulse scheme with linewidths and SNR measurements virtually identical to those obtained with prior methods. Residual water peaks with the intended amount of attenuation were observed in all cases. In the three patient studies for which the phase-

modulated dualband scheme was added to existing methods, the 40% reduction in peak RF power indicated by theory was confirmed in practice. For the dualband scheme, the peak power was far below the system limits, but for the pulse sequence using conventional PRESS pulses, the peak power neared system limits. The total power of these dualband pulses was calculated to be only slightly higher (1.11 times) than that of a typical 3.2 ms  $180^\circ$  slice-selective pulse. The specific absorption rate (SAR) for a patient MRSI acquisition using this pulse was calculated to be 1.37 W/kg and thus was far below FDA limits.

Overall, the spectral arrays appeared similar, with no apparent loss in quality with the new pulse sequence (Fig. 6). Quantitatively the calculated peak area ratios were virtually identical, with no significant differences. A total of 134 voxels were selected from the peripheral zones of the three patients and the (choline + creatine)/citrate ratio was calculated to be  $0.360 \pm 0.216$  from the dualband EPSE spectra and  $0.359 \pm 0.191$  for the data acquired with the prior method. For these same 134 voxels, ratios of the dualband CC/C values to the BASING values were calculated on a voxel-by-voxel basis. The mean ratio was  $1.01 \pm 0.26$ , indicating that both pulses produced similar results. To determine if there were significant differences in normal vs. abnormal tissues, the ratios were also calculated for the 100 voxels with normal metabolite levels ( $0.288 \pm 0.105$  for dualband,  $0.291 \pm 0.081$  for prior method) and for the eight voxels with abnormal metabolite ratios ( $0.900 \pm 0.350$  for dualband,  $0.817 \pm 0.239$  for prior method). No significant differences were detected. Furthermore, for the 134 voxels in these three patients, the mean choline SNR was  $9.65 \pm 4.65$  for the dualband spectra and  $9.05 \pm 4.14$  for the BASING spectra. The mean citrate SNR was  $39.31 \pm 22.63$  for the dualband and  $39.26 \pm 19.86$  for the BASING.

Figure 7 shows an example of imaging and spectroscopy results from a prostate cancer study using only the dualband pulses. This patient exam demonstrated a clear anatomic and metabolic abnormality in the left apical peripheral zone indicative of cancer. The lipid signals were nearly completely suppressed, and there were no baseline distortions. The 100-fold attenuation left a water peak approximately five times as intense as the citrate peak (Fig. 7c). The MRSI data were significantly different in the left midgland to the apex, which corresponded spatially with a positive histologic biopsy (Gleason grade 4 + 3). In the lesion, the choline resonance was greatly elevated and the citrate was reduced compared to the contralateral side. In Fig. 7, two voxels have been labeled in the axial  $T_2$ -weighted image: one healthy (H) and one indicative of cancer (C). The (choline + creatine)/citrate ratio in the healthy voxel was 0.3, whereas in the voxel centered on the lesion this ratio was 20.7. These altered metabolite ratios are typical for prostate cancer and agree with prior studies (1–4).

## DISCUSSION

Several different spectral-spatial, multidimensional pulse schemes have been applied to MRSI. One of the earliest, appropriately called spectroscopic imaging with multidimensional

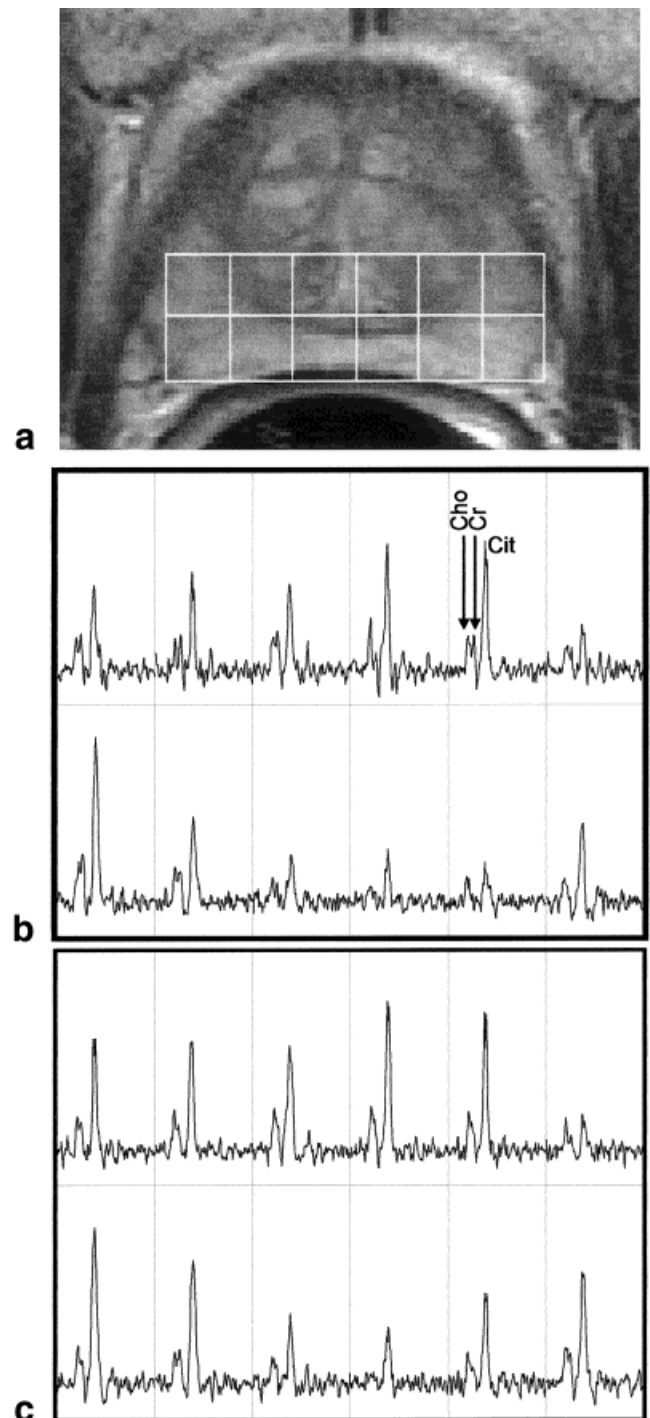


FIG. 6. Comparison of dualband EPSE MRSI with prior method. **a:** Axial  $T_2$ -weighted image of prostate, with MRSI grid overlaid. **b:** MRSI spectral data acquired using dualband EPSE pulses. **c:** MRSI spectral data acquired using the BASING scheme. The peak RF power was 40% lower for the EPSE MRSI method, with no loss in spectral quality.

dimensional pulses for excitation (SIMPLE), performed 3D localization by using a 2D spatial excitation followed by a slice-selective  $180^\circ$  pulse (9,24). More recently, spectral-spatial pulses have been exploited to build water and lipid suppression into the refocusing pulses of a PRESS se-

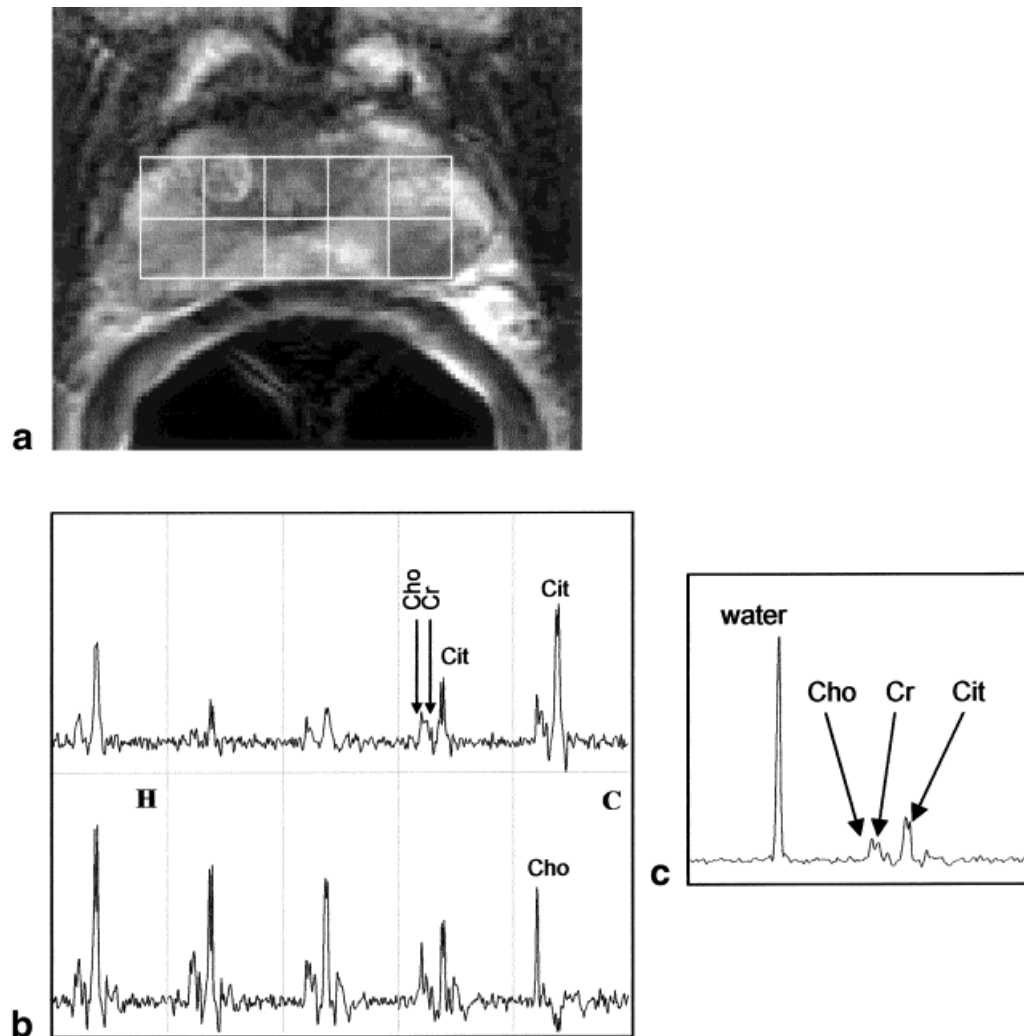


FIG. 7. **a:** Axial  $T_2$ -weighted image of the prostate of a 59-year-old cancer patient. **b:** Selected MRSI spectra (TR = 1000 ms, TE = 130 ms) acquired with the phase-modulated spectral-spatial dualband pulse scheme. The voxel labeled “C” displayed abnormally decreased citrate and increased choline, indicating the presence of cancer. The voxel labeled “H” (healthy tissue) demonstrated normal metabolite levels. **c:** The residual water signal was 5–10-fold higher than the metabolite resonance, and provided a valuable phase and frequency reference.

quence (22) with symmetric or asymmetric frequency profiles (25). The use of EPSE pulses in PRESS excitation has a number of significant advantages. First, EPSE pulses can be designed with very deep spectral nulls at the water frequency band fairly easily. Since this band is not refocused, water suppression does not degrade with  $B_1$  inhomogeneity and is not affected by  $T_1$  and  $T_2$  relaxation. In addition, the tolerance to  $B_0$  inhomogeneity is a design parameter that can be matched to the application. Another important feature of EPSE pulses is that chemical shift misregistration is negated since the spatial profile is not a function of frequency; therefore, the spatial profile is identical for all metabolites, unlike conventional slice-selective pulses.

In this project, we furthered the design of EPSE pulses for clinical MRSI studies in two significant ways. First, a dualband pulse was developed and implemented which allowed the independent, partial excitation of the water resonance while maintaining full excitation over the frequency range of the metabolites of interest—namely cho-

line, creatine, polyamines, and citrate. While designed for prostate MRSI, this method could also be applied for frequency ranges appropriate for other applications, such as brain spectroscopy. The second major goal of this project was the development of pulses with substantially reduced peak power requirements. This is particularly important for prostate MRSI, where selective excitation can be limited by the power restrictions inherent in body coil excitation. Due to the low duty-cycle for the MRSI acquisitions, the primary limitation is peak RF power, not total power deposited. The savings in peak power can also be used for increased spatial selectivity if desired.

The results of this study demonstrate the feasibility and clinical benefits of an MRSI sequence employing phase-modulated, dualband spectral-spatial pulses for prostate cancer studies. The PRESS sequence using dualband EPSE pulses provided improved spatial excitation compared to the prior BASING scheme (12), while providing a reduced, partially-excited residual water resonance. In both phantom and clinical MRSI exams, the attenuated water band

provided the intended degree of water suppression. The residual water peak provided a phase and frequency reference which can greatly benefit MRSI analysis by increasing the robustness of automatic postprocessing analysis techniques, thereby improving the accuracy and increasing the speed of data interpretation by reducing manual intervention. These dualband EPSE pulses, with their high spatial bandwidth and oscillating gradient lobes, also negated chemical shift misregistration errors. Uniform spectral data were produced without significant differences in the edge voxels. This can be critical for monitoring metabolite levels in cancerous or normal tissues close to the edges of the PRESS-selected region. This dualband scheme also passed prostate metabolite resonances with no loss in intensity, and, together with the spatial suppression pulses, provided robust lipid suppression for the clinical MRSI exams. Both frequency-based and location-based suppression schemes are required, since spatial suppression bands can not cover all the periprostatic lipids. However, they can suppress the adipose tissue near the rectum, which, due to magnetic susceptibility effects, can resonate at frequencies in the passband of the spectral-spatial pulses. The phase-modulation that was applied to the dualband EPSE pulses demonstrated significant reductions in peak power. The phase-modulated version of the dualband pulse required 40% less peak RF power than the original by theoretical calculations, and experimental results confirmed this power reduction.

In summary, new spectral-spatial RF excitation pulses were developed for clinical MRSI studies of the prostate. They were designed to provide both spatial and spectral selection, but unlike prior EPSE pulses, a dualband excitation scheme and additional phase-modulation was introduced to provide an amplitude-reduced residual water reference and to reduce peak power limits. These pulses were developed and tested in theoretical simulations before being evaluated in phantom and then clinical prostate MRSI studies. The pulse provided the desired improvements in spectral excitation, a dramatic reduction in peak RF power, and improved spatial selection as compared to prior non-EPSE excitation methods (BASING). The initial patient studies demonstrated substantial improvements, with no disadvantages, over current methods employed at our institution for clinical MRSI studies of prostate cancer.

## ACKNOWLEDGMENTS

The authors gratefully acknowledge helpful discussions and assistance from Drs. Ralph Hurd and Napapon Sailasuta from GE Medical Systems, and Dr. Sarah Nelson, Dr. Peter Carroll, Dr. Aliya Qayyum, Lucas Carvajal, Evelyn Proctor, Niles Bruce, and Gary Ciciriello from UCSF.

## REFERENCES

- Vigneron, D, Nelson, S, Kurhanewicz, J. Proton chemical shift imaging of cancer. In: Hricak H, Higgins CB, Helms CA, editors. *Magnetic resonance imaging of the body*. New York: Raven Press; 1997. p 205–220.
- Kurhanewicz J, Vigneron DB, Males RG, Yu K, Hricak H. In: Hricak H, Carroll PR, editors. *The prostate gland: radiologic clinics of North America*. Philadelphia: W.B. Saunders Co; 2000. p 115–138.
- Scheidler J, Hricak H, Vigneron DB, Yu KK, Sokolov DL, Huang LR, Zaloudek CJ, Nelson SJ, Carroll PR, Kurhanewicz J. Prostate cancer: localization with three-dimensional proton MR spectroscopic imaging-clinicopathologic study. *Radiology* 1999;213:473–480.
- Yu KK, Scheidler J, Hricak H, Vigneron DB, Zaloudek CJ, Males RG, Nelson SJ, Carroll PR, Kurhanewicz J. Prostate cancer: prediction of extracapsular extension with endorectal MR imaging and three-dimensional proton MR spectroscopic imaging. *Radiology* 1999;213:481–488.
- Bottomley PA. Spatial localization in NMR spectroscopy in vivo. *Ann NY Acad Sci* 1987;508:333–348.
- Moonen CT, von Kienlin M, van Zijl PC, Cohen J, Gillen J, Daly P, Wolf G. Comparison of single-shot localization methods (STEAM and PRESS) for in vivo proton NMR spectroscopy. *NMR Biomed* 1989;2: 201–208.
- Luyten PR, Marien AJ, den Hollander J. Acquisition and quantitation in proton spectroscopy. *NMR Biomed* 1991;4:64–69.
- Star-Lack J, Vigneron DB, Pauly J, Kurhanewicz J, Nelson SJ. Improved solvent suppression and increased spatial excitation bandwidths for three-dimensional PRESS CSI using phase-compensating spectral/spatial spin-echo pulses. *J Magn Reson Imaging* 1997;7:745–757.
- Spielman D, Meyer C, Macovski A, Enzmann D. 1H spectroscopic imaging using a spectral-spatial excitation pulse. *Magn Reson Med* 1991;18:269–279.
- Meyer CH, Pauly JM, Macovski A, Nishimura DG. Simultaneous spatial and spectral selective excitation. *Magn Reson Med* 1990;15:287–304.
- Pauly J, Spielman D, Macovski A. Echo-planar spin-echo and inversion pulses. *Magn Reson Med* 1993;26:776–782.
- Males RG, Vigneron DB, Star-Lack J, Falbo SC, Nelson SJ, Hricak H, Kurhanewicz J. Clinical application of BASING and spectral/spatial water and lipid suppression pulses for prostate cancer staging and localization by in vivo 3D 1H magnetic resonance spectroscopic imaging. *Magn Reson Med* 2000;43:17–22.
- Pickup S, Ding X. Pulses with fixed magnitude and variable phase response profiles. *Magn Reson Med* 1995;33:648–655.
- Shinnar M. Reduced power selective excitation radio frequency pulses. *Magn Reson Med* 1994;32:658–660.
- Le Roux P, Gilles RJ, McKinnon GC, Carlier PG. Optimized outer volume suppression for single-shot fast spin-echo cardiac imaging. *J Magn Reson Imaging* 1998;8:1022–1032.
- Shinnar M, Leigh JS. The application of spinors to pulse synthesis and analysis. *Magn Reson Med* 1989;12:93–98.
- Shinnar M, Bolinger L, Leigh JS. The synthesis of soft pulses with a specified frequency response. *Magn Reson Med* 1989;12:88–92.
- Shinnar M, Bolinger L, Leigh JS. The use of finite impulse response filters in pulse design. *Magn Reson Med* 1989;12:81–87.
- Shinnar M, Eleff S, Subramanian H, Leigh JS. The synthesis of pulse sequences yielding arbitrary magnetization vectors. *Magn Reson Med* 1989;12:74–80.
- Pauly J, Le Roux P, Nishimura D, Macovski A. Parameter relations for the Shinnar-Le Roux selective excitation pulse design algorithm. *IEEE Trans Med Imaging* 1991;10:53–65.
- Tran T-KC, Vigneron DB, Sailasuta N, Tropp J, Le Roux P, Kurhanewicz J, Nelson S, Hurd R. Very selective suppression pulses for clinical MRSI studies of brain and prostate cancer. *Magn Reson Med* 2000;43: 23–33.
- Star-Lack J, Nelson SJ, Kurhanewicz J, Huang LR, Vigneron DB. Improved water and lipid suppression for 3D PRESS CSI using RF band selective inversion with gradient dephasing (BASING). *Magn Reson Med* 1997;38:311–321.
- Moyher SE, Vigneron DB, Nelson SJ. Surface coil MR imaging of the human brain with an analytic reception profile correction. *J Magn Reson Imaging* 1995;5:139–144.
- Spielman D, Pauly J, Macovski A, Enzmann D. Spectroscopic imaging with multidimensional pulses for excitation: SIMPLE. *Magn Reson Med* 1991;19:67–84.
- Star-Lack JM, Adalsteinsson E, Gold GE, Ikeda DM, Spielman DM. Motion correction and lipid suppression for <sup>1</sup>H magnetic resonance spectroscopy. *Magn Reson Med* 2000;43:325–330.